Journal of Medicinal Chemistry

Article

pubs.acs.org/jmc

Inhibition of Homologous Recombination in Human Cells by Targeting RAD51 Recombinase

Fei Huang, Olga M. Mazina, Isaac J. Zentner, Simon Cocklin, and Alexander V. Mazin*

Department of Biochemistry and Molecular Biology, Drexel University College of Medicine, Philadelphia, Pennsylvania 19102, United States

Supporting Information

ABSTRACT: The homologous recombination (HR) pathway plays a crucial role in the repair of DNA double-strand breaks (DSBs) and interstrand cross-links (ICLs). RAD51, a key protein of HR, possesses a unique activity: DNA strand exchange between homologous DNA sequences. Recently, using a high-throughput screening (HTS), we identified compound **1** (B02), which specifically inhibits the DNA strand exchange activity of human RAD51. Here, we analyzed the mechanism of inhibition and found that **1** disrupts RAD51 binding to DNA. We then examined the effect of **1** on HR and DNA repair in the cell. The results show that **1** inhibits HR and increases cell sensitivity to DNA damage. We propose to use **1** for analysis of cellular functions of RAD51. Because DSB- and ICL-inducing agents are commonly used in anticancer therapy, specific inhibitors of RAD51 may also help to increase killing of cancer cells.

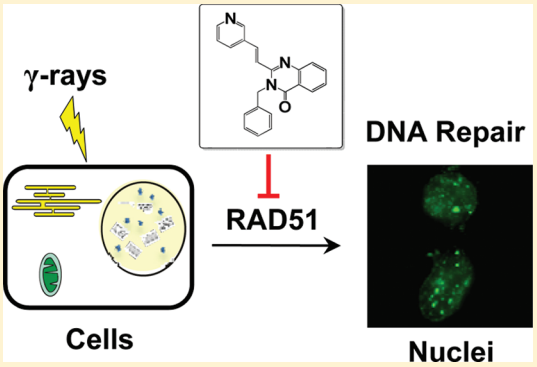

INTRODUCTION

The homologous recombination (HR) pathway plays an essential role in maintaining genome integrity in all organisms.[1,2] HR uses intact homologous DNA sequences to repair DNA double-strand breaks (DSBs) and interstrand cross-links (ICLs), the most harmful types of DNA lesions.[3,4]

The biochemical and genetic data indicate that HR initiates at the sites of DSBs. First, DNA ends of broken DNA are processed by exonucleases to generate protruding ssDNA tails.[5] Then Rad51, a key eukaryotic HR protein, binds to the ssDNA, forming the helical nucleoprotein filament.[6] The Rad51 filament carries out the search for homologous dsDNA and promotes DNA strand exchange, the basic step of HR.[7] DNA strand exchange results in formation of joint molecules, which provide both the template and the primer for DNA polymerase to retrieve genetic information that might be lost at the site of DSBs. Finally, joint molecules are resolved by action of branch migration enzymes and structure-specific nucleases.[8−10]

Mutations in Rad51 orthologs in yeast and bacteria cause high sensitivity to DNA-damaging agents.[1] In vertebrates, Rad51 is essential for cell viability; mouse and chicken Rad51$^{-/-}$ cells do not proliferate even in culture.[11,12] The essential function of vertebrate RAD51 complicates mutational analysis of this protein; only few hypomorphic Rad51 mutants have been analyzed so far, and they showed increased cell sensitivity to DNA-damaging agents.[13−15]

Here, we propose to develop specific small-molecule inhibitors of human RAD51 that can be used for the analysis of the RAD51 cellular functions and the mechanism of DNA strand exchange in vitro. RAD51 inhibitors may also help to increase cancer cell sensitivity to chemo- and radiotherapy because many anticancer therapies involve agents that induce DSBs and ICLs, e.g., ionizing radiation (IR) or *cis*-diamminedichloroplatinum(II) (cisplatin), which are repaired by HR.[16] Small-molecule inhibitors offer substantial advantages over both siRNA inhibition and antibody microinjection.[17] Because small-molecule inhibitors act reversibly and quickly, with diffusion likely to be the rate-limiting step, they can be applied at specific points of cell cycle or organism development. They may target individual protein domains, thereby helping to link specific biochemical activities with the protein functions in the cell. The ability to inhibit proteins transiently and dose-dependently makes small-molecule inhibitors especially valuable for studying proteins that are essential for cell viability, like RAD51.

Several small-molecule RAD51 inhibitors have been described.[18,19] However, they lack specificity for RAD51 and can be used only for in vitro studies of Rad51 activities. Recently, we identified a specific inhibitor of the RAD51 DNA strand exchange activity, **1** (B02) (Figure 1a), by screening the NIH Small Molecule Repository of ~200 000 compounds.[20] In the current work, we analyze the mechanism of inhibition and demonstrate that **1** acts by disrupting RAD51 binding to DNA and formation of the nucleoprotein filament. Furthermore, we show that **1** has a substantial effect on HR and DNA repair in human and mouse cells. Our results show that **1** inhibits DSB-induced HR and increases cell sensitivity to ICL agents cisplatin

Received: September 5, 2011
Published: March 1, 2012

dx.doi.org/10.1021/jm201173g | J. Med. Chem. 2012, 55, 3011−3020

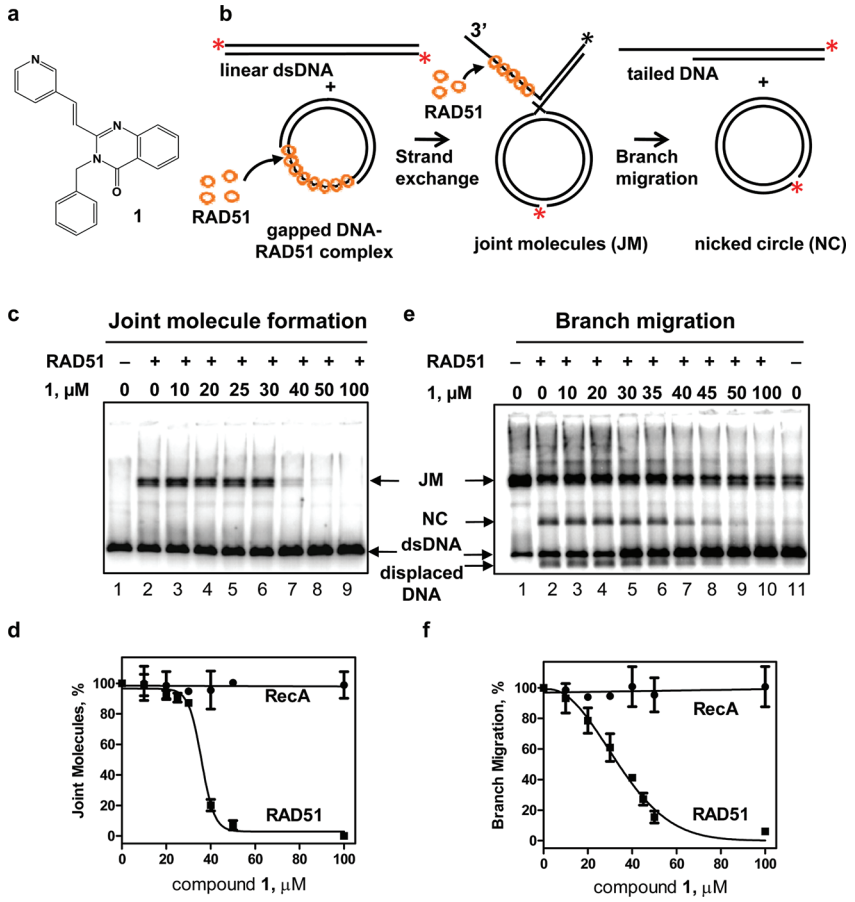

Figure 1. Compound **1** specifically interacts with RAD51 and inhibits its activities. (a) Structure of the compound **1**. (b) Scheme of the DNA strand exchange and branch migration assays. The asterisk denotes the ^{32}P label. (c) Effect of **1** (10−100 μM) on the DNA strand exchange activity of RAD51. (d) The yield of RAD51- and RecA-generated joint molecules (JM) was plotted as a graph. (e) Effect of **1** (10−100 μM) on the branch migration activity of RAD51. Lanes 1 and 11 represent JMs before and after 8 h of incubation in the absence RAD51, respectively. (f) The yield of the RAD51- and RecA-generated nicked circle (NC) product was plotted as a graph. The extent of JM and NC formation in the absence of **1** was expressed as 100%. The actual extent was 32% and 15% of JM (relative to linear dsDNA) and 21% and 63% of nicked circles for RAD51 and RecA (relative to JM substrate), respectively. Controls containing no RAD51 are shown in lane 1. Experiments were repeated at least three times. Error bars represent standard deviation (SD).

and mitomycin C (MMC). These data show that specific RAD51 inhibitors may be instrumental for the analysis of RAD51 activities and cellular functions and for development of combination anticancer therapies.

RESULTS

Compound 1 Binds Specifically to RAD51 and Inhibits Its Activities. RAD51 and its *Escherichia coli* homologue RecA possess DNA strand exchange and DNA branch migration activities.[7] We wished to examine the effect of **1** (Figure 1a) on these activities of both proteins.

We used pBSK (+) gapped and linear dsDNA substrates that allow separate analysis of DNA strand exchange and branch migration promoted by RAD51/RecA (Figure 1b).[7] At the first step, RAD51/RecA promotes DNA strand exchange between gapped DNA and linear DNA substrates, resulting in formation of joint molecules. Joint molecules were then purified and used as substrates for RAD51/RecA branch migration. In accord with our previous data that showed specific inhibition of RAD51 by **1** in the D-loop assay,[20] we observed that **1** (10−100 μM) inhibited DNA strand exchange promoted by RAD51 (Figure 1c,d) but not by RecA (Figure 1d, Supporting Information Figure 1b). We then found that **1** (10−100 μM) inhibited the DNA branch migration activity of RAD51 (Figure 1e,f). The inhibition was specific, as **1** did not inhibit the branch migration activity of RecA (Figure 1f, Supporting Information Figure 1c). The IC_{50} of RAD51 inhibition by **1** was 35 μM for both DNA strand exchange and DNA branch migration. We then tested whether RAD51 inhibition is caused by the direct interaction of **1** with RAD51. Using the surface plasmon resonance (SPR) technique, we demonstrated that **1** (6.25−50 μM) binds to RAD51 but not to RecA (Figure 2, Supporting Information Figure 2). For **1** binding to RAD51 in the absence of ATP, kinetic values are as follows: $k_a = (4.5 \pm 0.3) \times 10^3$ M^{-1} s^{-1}; $k_d = (2.5 \pm 0.3) \times 10^{-2}$ s^{-1}; $K_d = 5.6$ μM. Previously, we showed using the ethidium bromide displacement assay that **1** does not bind DNA.[20] Thus, **1** inhibits DNA strand exchange and branch migration activities through direct and specific binding to RAD51.

Compound 1 Inhibits Formation of the RAD51-ssDNA Filament. We wished to explore the mechanism of RAD51 inhibition by **1**. First, we performed the order-of-addition experiment, in which **1** (20 μM) was added either to the RAD51-ssDNA filament (I) or to free RAD51 prior to filament formation (II) (Figure 3a). The effect of **1** on the RAD51 strand exchange activity was measured using the D-loop assay.

dx.doi.org/10.1021/jm201173g | J. Med. Chem. 2012, 55, 3011−3020

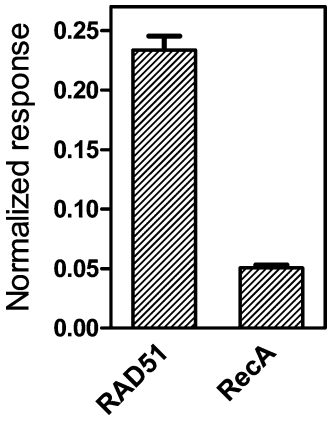

Figure 2. Compound **1** binds directly to RAD51. **1** (50 μM) was injected onto a sensor chip to which Rad51 or RecA had been immobilized. The running buffer S was supplemented with ATP (100 μM). Responses to **1** were normalized to the theoretical maximum response of the surface (R_{max}), assuming a 1:1 interaction. Experiments were repeated at least three times. Error bars represent SD.

The results show that the inhibitory effect was substantially stronger when **1** was incubated with free RAD51 (II) (Figure 3b,c), suggesting that **1** inhibits RAD51 binding to ssDNA during nucleoprotein filament formation.

Then we examined the effect of **1** on RAD51 binding to ssDNA directly using the electrophoresis mobility shift assay. We measured the effect of **1** (25 μM) on the ability of RAD51-ssDNA complexes to withstand increasing concentrations of NaCl that destabilize protein−DNA interactions.[21] We found that **1** indeed inhibited DNA binding by RAD51, as in the presence of **1**, formation of RAD51 complexes with a 90-mer ssDNA (oligo 90) (Supporting Information Table 1) substantially decreased (Figure 4a,b). Consistent with inhibition of DNA binding, **1** also inhibited ATP hydrolysis by RAD51, which depends on ssDNA binding (Figure 4c).

Formation of nucleoprotein filaments involves binding of RAD51 monomers to ssDNA and also interactions between RAD51 monomers. These monomer−monomer interactions are responsible for RAD51 oligomerization in solution. We examined the effect of **1** (200 μM) on RAD51 oligomerization using gel filtration on a Superose 6 column (GE Healthcare) (Supporting Information Figure 3). We found that **1** did not affect the spectrum of RAD51 oligomers, which ranged from 590 kDa (~16-mers) to 150 kDa (~tetramers).

Thus, the results showed that **1** inhibits RAD51 binding to ssDNA, an essential step of DNA strand exchange and branch migration promoted by this protein. Furthermore, **1** likely inhibits RAD51-DNA interactions rather than monomer−monomer interactions.

Compound 1 Disrupts Binding of dsDNA to RAD51-ssDNA Filament. The proteins of the RAD51/RecA protein family possess two DNA-binding sites.[22,23] The primary site binds ssDNA during the assembly of RAD51/RecA-ssDNA filaments. The secondary site binds dsDNA during the search for homology. Binding of long (several kbp) dsDNA molecules may encompass several secondary sites on different RAD51-ssDNA filaments, resulting in formation of coaggregates (Figure 4d) that can be sedimented by low-speed centrifugation.[24] Here, we tested the effect of **1** on formation of coaggregates as a gauge of dsDNA binding to the secondary RAD51 site. Coaggregation was carried out by incubating the

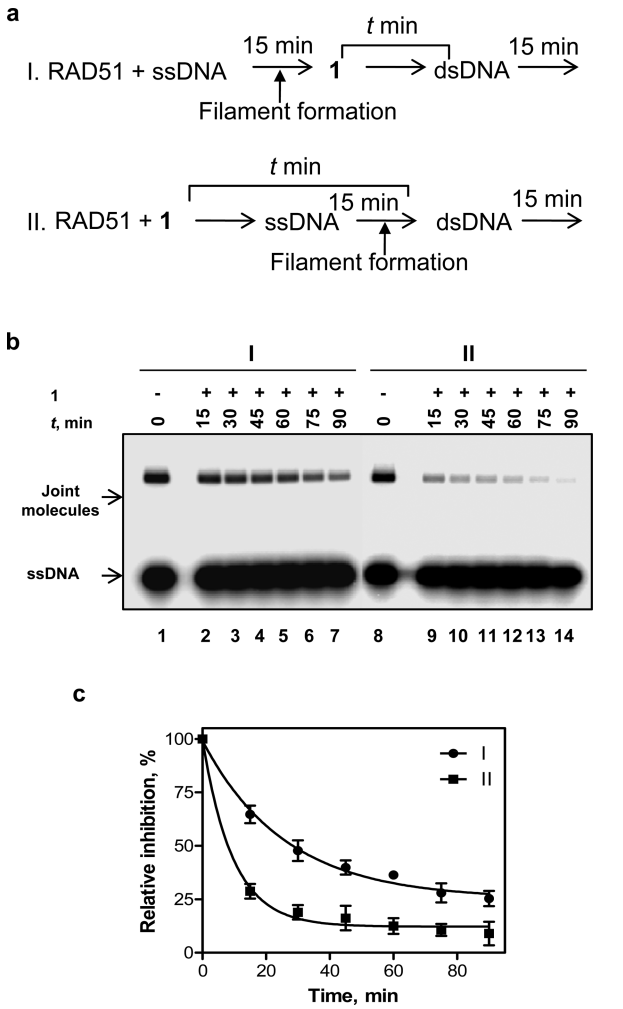

Figure 3. The order of compound **1** addition affects the efficiency of D-loop formation promoted by RAD51. (a) Order of addition of **1**. The numbers above the arrows indicate time of incubation. **1** (20 μM) was added either to the RAD51-ssDNA filament (I) or to RAD51 before addition of ssDNA (II). (b) The joint molecules were analyzed by electrophoresis in a 1% agarose gel. (c) The relative inhibition of joint molecule formation by **1** is expressed as the ratio of the joint molecules formed by RAD51 that was treated with **1** to those formed by RAD51 that was not treated with **1**. "*t*" denotes the time period between the addition of **1** and dsDNA. Experiments were repeated at least three times. Error bars represent SD.

RAD51-ssDNA filament with ^{32}P-labeled pUC19 dsDNA (linearized by BamHI). The stability of coaggregates was measured by their ability to withstand elevated NaCl concentrations.[25,26] We found that treatment of the RAD51-ssDNA filament with **1** (20 μM) severely reduced formation of coaggregates with dsDNA even at low NaCl concentrations (Figure 4e). This result shows that **1** disrupts dsDNA binding to the secondary RAD51 site. This disruption may account for a relatively moderate inhibition of DNA strand exchange in the order-of-addition experiments protocol II (Figure 3) when **1** was added after completion of filament formation.

Compound 1 Disrupts the RAD51 Foci Formation. We wished to test whether **1** can inhibit RAD51 activities in the cell. In response to DNA damage, RAD51 accumulates in distinct nuclear structures known as foci.[27] Because RAD51 foci colocalize with ssDNA formed in the cell after DNA damage, it is thought that the foci represent RAD51 complexes with DNA

dx.doi.org/10.1021/jm201173g | J. Med. Chem. 2012, 55, 3011−3020

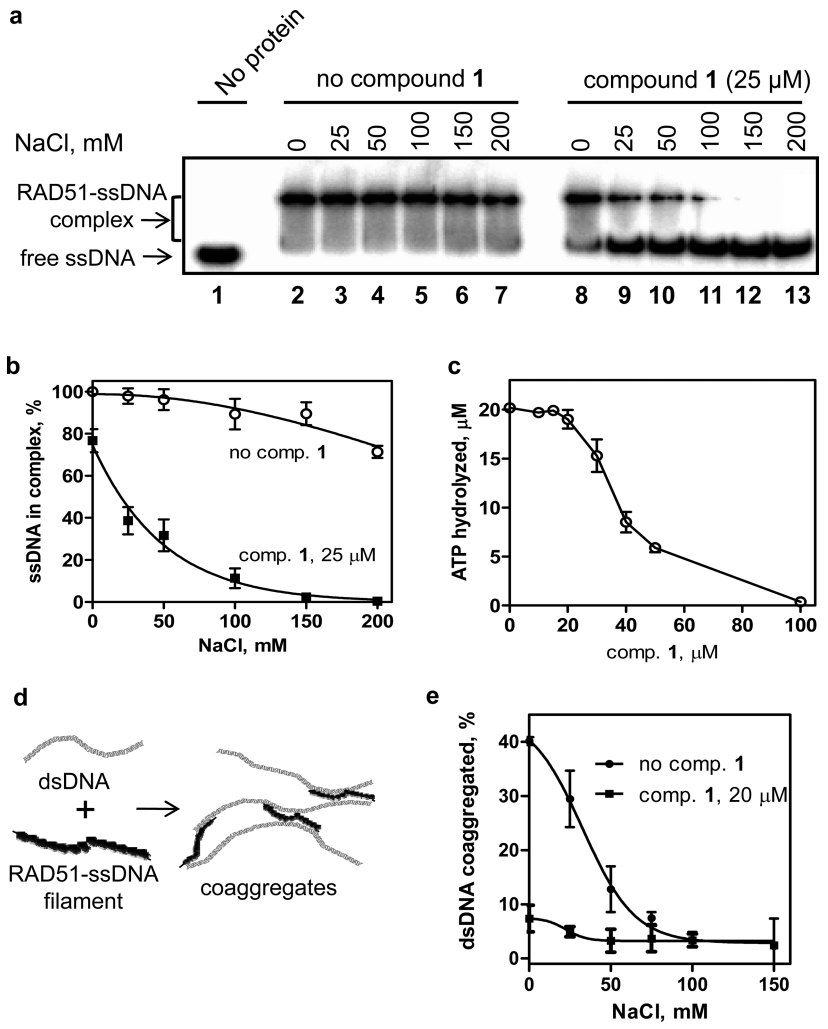

Figure 4. Compound **1** inhibits DNA binding by RAD51. (a) Effect of **1** (25 μM) on binding by RAD51 to a 90-mer ssDNA (oligo 90). (b) The results in (a) are shown as a graph. (c) Effect of **1** (0–100 μM) on ATP hydrolysis by RAD51. The result is shown as a graph. (d) Scheme of the dsDNA coaggregation assay. (e) Effect of **1** (20 μM) on formation of coaggregates between the RAD51-ssDNA filament and ^{32}P-labeled linear pUC19 dsDNA (linearized by BamHI). Experiments were repeated at least three times. Error bars represent SD.

repair intermediates.[28] If **1** inhibits DNA binding of RAD51 in the cell, one may expect a decrease in RAD51 foci formation. Indeed, we found that **1** inhibited RAD51 foci formation induced in 293 human embryonic kidney (HEK) cells by IR. In the presence of **1** (50 μM), the fraction of cells with RAD51 foci ($\geq$1 focus) was decreased 3.8-fold, from 72 $\pm$ 10% to 19 $\pm$ 6%, almost to the level of foci formation observed in nonirradiated cells (15 $\pm$ 13%) (Figure 5a,b); the average number of RAD51 foci per nucleus decreased 4.4-fold, from 53 $\pm$ 11 to 12 $\pm$ 4 (Figure 5c). At lower concentrations (20 μM), **1** also inhibited IR-induced RAD51 foci formation; however, the inhibitory effect was smaller (F. Huang and A. Mazin, unpublished observation).

Compound 1 Inhibits DSB-Induced HR in Human Cells. We then examined whether **1** suppresses DSB-induced HR in human cells. We monitored HR events using the chromosomally integrated DR-GFP reporter.[29] The DR-GFP construct consists of two defective copies of the *GFP* gene encoding green fluorescent protein (GFP), the *SceGFP* that is disabled by insertion of an 18-bp recognition site for I-SceI endonuclease and the *iGFP* that is truncated at both ends (Figure 6a). A unique DSB is generated in this construct after the cells are transfected with pCBASce plasmid that encodes I-SceI endonuclease. The repair of this DSB by HR that occurs between two *GFP* copies gives rise to a functional *GFP* gene. Thus, each HR event can be scored by the appearance of a green fluorescent cell.

We found that **1** reduces formation of GFP-positive cells in a concentration dependent manner; the reduction was approximately 8-fold at 20 μM **1** (Figure 6b, panels 2–5; Figure 6c). In control experiments, we found no effect of **1** on GFP expression or on recovery of GFP-positive cells when HEK cells were transfected with pMX-GFP plasmid encoding GFP (Figure 6d). Also, using Western blotting we observed no detectable effect of **1** on the expression level of I-SceI or RAD51 in HEK-GFP cells, which could affect the efficiency of HR through mechanisms unrelated to RAD51 inhibition (Supporting Information Figure 4). To ensure that the observed inhibition is not due to a nonspecific poisoning of HR by a hydrophobic agent, we used (1*R*)-4,7,8,11,11-pentamethyl-1,2,3,4-terahydro-1,4-methanophenazine-1-carboxylic acid (A12) which has the hydrophobicity level (log *P* = 3.9) similar to that of **1** (log *P* = 3.7) but did not inhibit significantly the DNA strand activity of RAD51.[20] We found that in the tested range of concentrations (5–20 μM) **2** (A12) did not inhibit formation of GFP-positive cells (Figure 6c). Taken

dx.doi.org/10.1021/jm201173g | J. Med. Chem. 2012, 55, 3011–3020

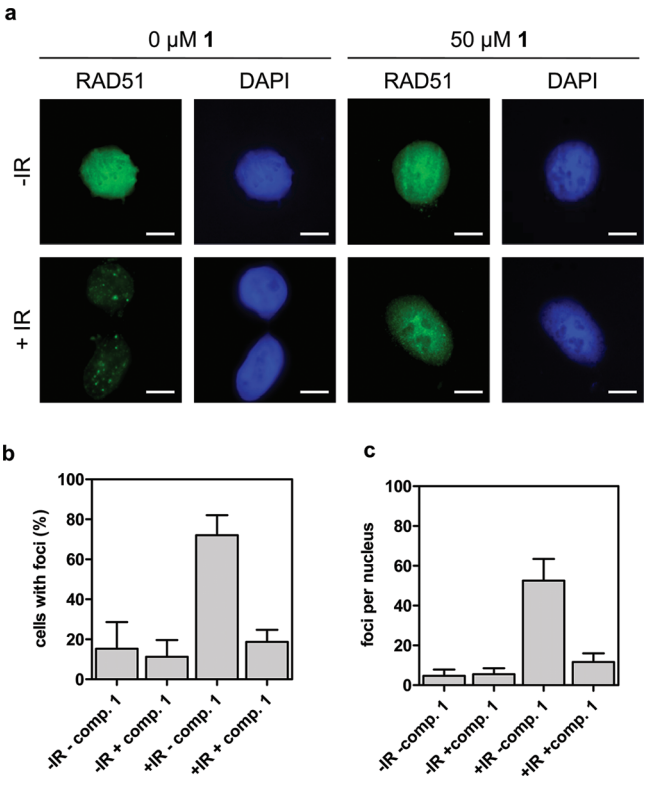

Figure 5. Compound **1** disrupts the RAD51 foci formation. (a) HEK cells were exposed to 0.5 Gy of IR in either the presence (50 μM) or the absence of **1**. RAD51 foci were visualized by immunostaining using RAD51 antibodies. Nuclei were counterstained with DAPI. Bars indicate 20 μm. (b) The fraction of foci-positive cells (the cells with $\geq$1 focus) was determined by counting at least 150 cells in each experiment. (c) The mean of foci number per nucleus in foci- positive cells was determined by counting at least 50 cells in each experiment. Experiments were repeated three times. Error bars represent SD.

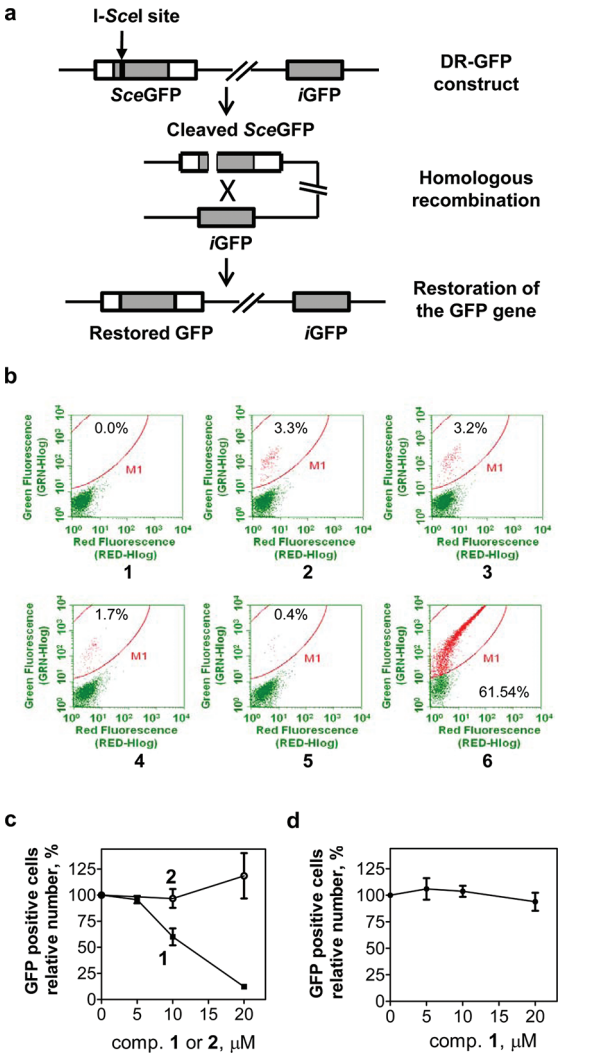

Figure 6. Compound **1** inhibits DSB-induced HR in human cells. (a) Scheme of HR at the DR-GFP locus. (b) The effect of **1** on HR at the DR-GFP induced by I-SceI-DSBs was determined using flow cytometry. Green fluorescence (GRN-Hlog) was plotted against red fluorescence (RED-Hlog) for the sample of 10 000 cells. The GFP-positive population is denoted by the elliptical M1 marker. Parental cells untransformed with I-SceI were used as a negative control (panel 1). Cells with I-SceI-induced DSBs were either untreated (panel 2) or treated with **1** at 5, 10, or 20 μM (panels 3–5). Parental cells that were transfected with pMX-GFP plasmid encoding GFP protein were used as a positive control (panel 6). (c) Effect of **1** (squares) and **2** (open circles) on the efficiency of formation GFP-positive cells shown as a graph (the data for **1** are from panel b). (d) Effect of **1** on the efficiency of formation of GFP-positive cells after transfection with pMX-GFP-plasmid. The efficiency of formation of GFP-positive cells that were untreated with **1** or **2** was expressed as 100%. Experiments were repeated at least three times. Error bars represent SD.

together, our results show that **1** reduces the level of DSB-induced HR, consistent with inhibition of the RAD51 activity in human cells.

Compound 1 Increases Cell Sensitivity to DNA-Damaging Agents. We examined whether **1** can enhance cell sensitivity to DSB- and ICL-inducing anticancer agents cisplatin and MMC. Using the clonogenic survival assay, we found that in the presence of **1** (5 μM) mouse embryonic fibroblasts (MEF) became approximately 17- and 5-fold more sensitive to cisplatin (32 μM) and MMC (1 μM), respectively (Figure 7a,b). Because p53 protein is commonly mutated in many human cancers, we also tested the effect of **1** on $Tp53^{-/-}$ MEF. We found that the sensitivity of $Tp53^{-/-}$ MEF to cisplatin and MMC increased in the presence of **1** similar to wild type cells (Supporting Information Figure 5). In these experiments, we used 5 μM **1**, a concentration at which **1** alone did not have a substantial effect on the viability of wild type or $Tp53^{-/-}$ MEF (Figure 7c). We suggested that the inhibitory effect of **1** on cell survival observed in co-treatment experiments was due to depletion of RAD51 that translocated to the sites of DNA damage. We tested this proposal using HEK cells in which the RAD51 expression level was decreased by siRNA (Supporting Information Figure 6). Our results show that indeed combination of specific RAD51 siRNA and **1** more strongly sensitized HEK cells to cisplatin than did each of these reagents alone (Figure 7d). We also determined the minimum incubation time with **1** that was required for cells' sensitization for cisplatin. Our data indicate that 10–12 h of incubation was required to increase the sensitivity of HEK cells for cisplatin (Figure 7e). After 16 h, the maximal sensitivity was reached. Thus, **1** causes cell sensitization to cisplatin and MMC, indicating the ability of **1** to inhibit RAD51-dependent DSB repair in the cell.

Compound 1 Increases Cell Sensitivity to PARP1 Inhibitors. Poly(ADP-ribose) polymerase 1 (PARP1) is involved in repair of ssDNA breaks. Inhibition of PARP1 leads to generation of DSBs during DNA replication, which is

dx.doi.org/10.1021/jm201173g | J. Med. Chem. 2012, 55, 3011–3020

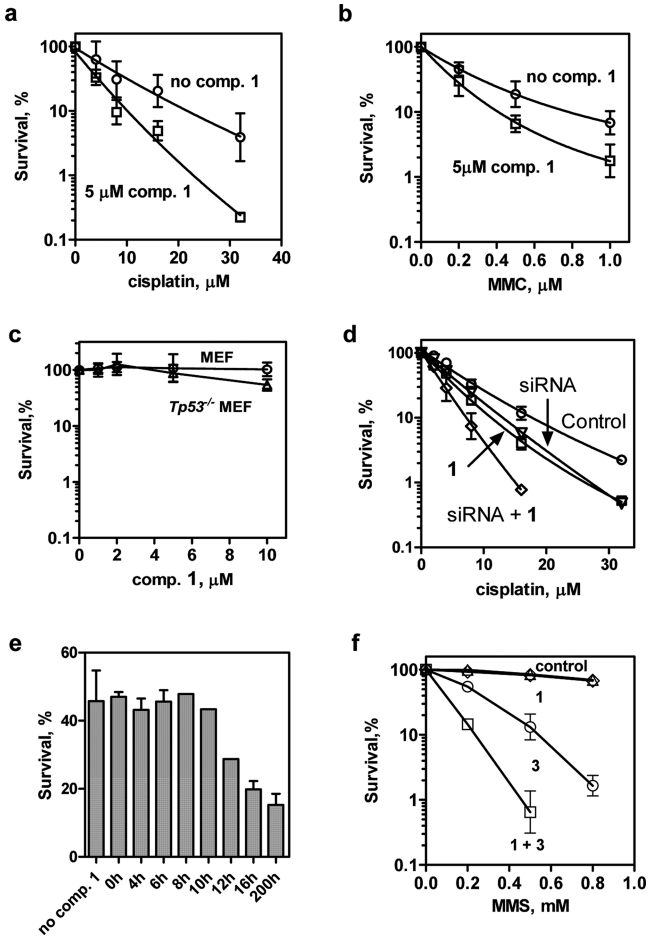

Figure 7. Compound **1** increases cell sensitivity to DNA-damaging agents. (a, b) Survival of MEF treated with cisplatin or MMC for 1 h in the absence or presence of **1** (5 μM). (c) Effect of **1** on survival of MEF and *Tp53*$^{-/-}$ MEF. (d) Effect of **1** (0−10 μM) and RAD51 siRNA on HEK cells' sensitivity to cisplatin. HEK cells were transfected with RAD51 siRNA and incubated 40 h before treatment with cisplatin at indicated concentrations and **1** (5 μM). (e) Effect of **1** incubation time with HEK on cell sensitivity to cisplatin. HEK cells were treated with **1** (5 μM) for 1 h followed by addition of cisplatin (16 μM) and incubation for 1 h. Then cisplatin was removed and cells were incubated with **1** (5 μM) for the indicated times followed by medium replacement and additional incubation for 7−10 days. (f) Effect of **3** (0.01 μM) and **1** (5 μM) on MEF sensitivity to MMS. Experiments were repeated at least three times. Error bars represent SD.

lethal in HR-deficient cells.[16] If **1** indeed inhibits RAD51-dependent HR in the cell, one can suggest that combination of **1** with PARP1 inhibitors would more strongly sensitize cells to DNA-damaging agents than would each of these reagents alone. To induce DNA damage, we used methyl methanesulfonate (MMS). As expected, PARP1 inhibitor **3** (4-[3-(4-cyclopropanecarbonylpiperazine-1-carbonyl)-4-fluorobenzyl]-2*H*-phthalazin-1-one (AZD2281))[30] (0.01 μM) strongly increased the sensitivity of MEF to MMS (Figure 7f). In contrast, **1** (5 μM) did not increase MEF sensitivity to MMS at the tested concentrations. However, combination of **1** with **3** rendered MEF extremely sensitive to MMS, consistent with inhibition of HR by **1** in the cell.

DISCUSSION AND CONCLUSIONS

Development of inhibitors of DNA repair proteins has been recently recognized as a therapeutic strategy against cancer and as a novel approach for analysis of DNA repair pathways. The HR pathway plays an import role in the repair of DSBs and ICLs. It was shown that down-regulation of human RAD51, a key HR protein, with siRNA[31−33] or its inactivation by mutations[13,14] greatly reduces the efficiency of DNA repair, increasing cell sensitivity for DSB- and ICL-induced agents. Previously, by screening the NIH Small Molecule Repository, we identified the first specific small-molecule inhibitor of RAD51, termed **1**.[20] Here, we analyze the mechanism of RAD51 inhibition by **1** and its ability to inhibit RAD51 homologous recombination and DNA repair in cells. We demonstrate that **1** binds to RAD51 and inhibits its DNA strand exchange and branch migration activities with high specificity, as it does not affect *E. coli* RecA, a structural and functional homologue of RAD51. Importantly, our results demonstrate that **1** inhibits RAD51-dependent HR events in the cell and promotes cell killing by cytotoxic DSB- and ICL-inducing agents.

Because the RAD51-ssDNA filament plays a critical role in HR, its formation is tightly regulated by various factors that either enhance or inhibit RAD51 binding to ssDNA.[34−36] Our data demonstrated that **1** also inhibits RAD51 filament formation. Filament formation involves two steps: formation of short initial complexes, which is driven mainly by protein−DNA interaction between RAD51 monomers and ssDNA, and filament elongation, which relies on interactions between RAD51 monomers.[37] Our results showed that **1** impairs RAD51 filament formation by targeting protein−DNA interactions. The filament formation involves binding ssDNA to the RAD51 primary site. We found using a coaggregation assay that **1** also inhibits dsDNA binding to the secondary RAD51 site, which normally occurs during the search for homology.[6] The observed inhibition of DNA binding by **1** to both the primary and the secondary site is not entirely surprising because these sites are located in proximity to the protein structure and may partially overlap.[38]

The important question was whether **1** inhibits RAD51-dependent HR and DNA repair in the cell. To address this question, we carried out several cell-based assays. First, we found that **1** inhibited formation of RAD51 foci in response to IR, which is thought to reflect RAD51 accumulation at the sites of damaged DNA and formation of RAD51-DNA complexes during recombinational DNA repair.[28,39] Then using a chromosomally integrated GFP reporter,[29] we showed that **1** decreased, up to 8-fold, the frequency of DSB-induced HR in human cells. Also, we demonstrated that **1** increases cell sensitivity to ICL- and DSB-inducing agents cisplatin and MMC. This result is consistent with previous reports that showed high sensitivity of human and mouse cells for cytotoxic agents, e.g., IR, MMC, or cisplatin, when RAD51 was depleted by siRNA or inactivated by mutations.[14,31,32] Finally, we found that combination of **1** with PARP1 inhibitor **3** increases cell sensitivity to an alkylating agent (MMS) much more than does **3** alone. PARP1 inhibitors disrupt the repair of ssDNA breaks, leading to generation of DSBs during DNA replication.[16] Because inhibition of PARP1 is lethal in HR-deficient cells, PARP1 inhibitors were successfully used for killing breast cancer cells in which HR proteins BRCA1 and BRCA2 are mutated. Our finding that PARP1 inhibitors enhance the effect

dx.doi.org/10.1021/jm201173g | *J. Med. Chem.* 2012, 55, 3011−3020

of **1** on cell sensitivity to DNA damage is fully consistent with inhibition of HR by **1**. In the co-treatment experiments, **1** showed activity at concentrations lower (5 μM) than in other biological assays probably because of the depletion of RAD51 that accumulates at the sites of DNA damage. Indeed, we found that depletion of RAD51 with siRNA has an additive effect with **1** treatment. Also, IC_{50} values in vitro depend on the protein concentration, making it difficult to compare them directly to values obtained in cells.[40] Moreover, RAD51 is not a canonical enzyme; the DNA strand exchange assay requires rather high RAD51 concentrations (stoichiometric relative to DNA substrates). Concerning RAD51 foci formation, it is worth noting that each RAD51 focus involves thousands of RAD51 monomers; therefore, a decrease in their number in each focus may not be readily detectable by immunostaining and requires higher **1** concentrations (20−50 μM). Overall, our results demonstrate that **1** inhibits RAD51-dependent HR and DSB repair in mammalian cells (Figure 8).

Because small-molecule inhibitors can be applied in a cell cycle and in a concentration- dependent manner, they are especially useful for analysis of proteins essential for cell viability, like RAD51. By applying **1** for different periods of time after DNA damage by cisplatin, we were able to determine a maximal time for which DNA repair can be delayed before the cells start dying. RAD51 inhibition is fully reversible up to 10 h after DNA damage, after which cell lethality increases sharply, approaching a maximum after 16 h. This timing likely reflects the check point capability to delay cell entry into S phase, in which RAD51 function is thought to be critically important for cell survival.[41]

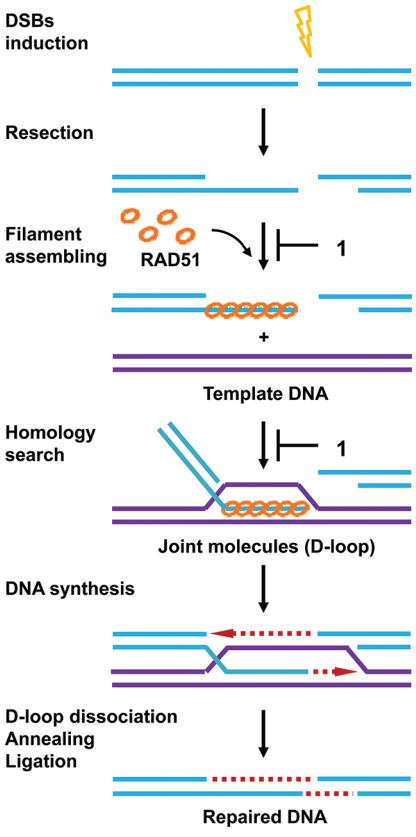

Figure 8. Compound **1** inhibits HR by disrupting RAD51 binding to DNA. During the repair of DNA double-strand breaks, RAD51 binds to ssDNA, forming the nucleoprotein filament. The filament searches for homologous dsDNA sequence to form joint molecules. The homologous DNA then is used as a template for DNA polymerase. Dissociation of the joint molecules and reannealing of DNA ends lead to the restoration of the DNA structure. **1** inhibits HR by disrupting formation of the RAD51-ssDNA filament and interaction of the filament with dsDNA during the search for homology.

Development of small-molecule inhibitors of DNA repair enzymes has became an important strategy to improve radio- and chemotherapy treatment of cancer.[42] Our results indicate that combination of inhibitors that target alternative DNA repair pathways, e.g., RAD51-dependent and PARP1-dependent DNA repair, can be especially efficient for sensitizing cancer cells for radio- and chemotherapeutic agents. Targeting RAD51 may represent an important strategy to specifically eradicate cancer cells. Studies with siRNA show that inhibition of RAD51 renders cancer cells more vulnerable than normal cells to radio- and chemotherapeutic agents.[31] It was suggested that RAD51-dependent HR represents a mechanism that compensates for the loss of other DNA repair pathways often occurring in cancer cells owing to genome instability.[31] For instance, Polβ, a member of the base excision repair (BER) pathway, is altered in approximately 30% of human tumors.[43] In BER-deficient cells, unrepaired DNA intermediates convert to DSBs during DNA replication, exposing cancer cells to a greater than normal cell dependence on HR.[44] Consistent with the compensatory role that HR may play in cancer cells, RAD51 was found to be overexpressed in many tumors.[45−47]

Our results demonstrate that **1** inhibitor of RAD51 can efficiently suppress DSB- dependent HR in the cell. The inhibitor can be used for the analysis of RAD51 cellular functions and for development of novel anticancer therapies.

EXPERIMENTAL SECTION

Chemicals, Proteins, and DNA. **1** was purchased from Ryan Scientific. Cisplatin, MMC, and MMS were purchased from Sigma-Aldrich. **3** was purchased from Selleck Chemicals. Human RAD51 and replication protein A (RPA) were purified as described.[21,48] *E. coli* RecA was purchased from USB, Inc. The oligonucleotides (Supporting Information Table 1) were purchased from IDT, Inc. and further purified by electrophoresis.[49,50] Plasmid DNA was purified using Qiagen kits. Gapped DNA was prepared by annealing the pBSK (+) XhoI-AlwNI fragment (2065 bp) to pBSK (+) ssDNA and purified as described previously.[50] All DNA concentrations are expressed as moles of nucleotide.

Purity. Purity values for all tested compounds were found to be above 95% from the high-performance liquid chromatography (HPLC) analyses (Column Wasters Symmetry C18, 5 μm, 75 mm × 4.6 mm; UV detection, 254 and 215 nm; eluent acetonitrile/water with gradient elution starting with 35% acetonitrile; 0.6 mL/min).

Cell Culture. MEF samples were from American Type Culture Collection (ATCC). *Tp53*$^{-/-}$ MEF was a kind gift from Dr. Astrinidis. HEK cells with the chromosomally integrated DR-GFP reporter (HEK-GFP) were kindly provided by Dr. Clifford.[29] Cells were maintained in Dulbecco modified Eagle medium+ (DMEM+) composed of DMEM (Sigma) supplemented with 10% fetal bovine serum (FBS) (Invitrogen), penicillin (100 units mL^{-1}), and streptomycin (100 μg mL^{-1}) in the presence of 5% CO_2 at 37 °C.

Joint Molecule Formation Assay. For RAD51-promoted reaction, RAD51 (1 μM) was incubated with **1** in the indicated concentrations in buffer containing 25 mM Tris acetate, pH 7.5, 2 mM ATP, 275 mM NaCl, 1 mM $MgCl_2$, 1 mM $CaCl_2$, 1 mM DTT, and 100 μg/mL BSA for 30 min at 37 °C, and then pBSK (+) gapped DNA (4 μM, nt) was added to form nucleoprotein filaments for 15 min. RPA (80 nM) was added to the mixture followed by a 10 min incubation. Joint molecule formation was initiated by addition of 5′-

dx.doi.org/10.1021/jm201173g | J. Med. Chem. 2012, 55, 3011−3020

labeled linear pBSK (+) dsDNA (4 μM, nt) (linearized by XhoI) and carried out for 2 h.

For RecA-promoted reaction, RecA (1 μM) was incubated with indicated concentrations of **1** in buffer containing 33 mM Tris HCl, pH 7.5, 3 mM ATP, 15 mM $MgCl_2$, 2 mM DTT, 100 μg/mL BSA, 10 mM phosphocreatine, and 10 units/mL creatine phosphokinase for 30 min at 37 °C, and then pBSK (+) gapped DNA (5 μM, nt) was added to form the nucleoprotein filaments for 10 min. Joint molecule formation was initiated by addition of 3′-labeled linear pBSK (+) dsDNA (4 μM, nt) (linearized by AlwNI) and single-stranded DNA binding protein (SSB) (82.5 nM) protein and carried out for 20 min.

In RAD51 and RecA-promoted reactions, joint molecules were deproteinized by addition of SDS to 1% and proteinase K to 880 μg mL^{-1} and incubation for 15 min at 37 °C. Then 0.1 vol of loading buffer (70% glycerol, 0.1% bromophenol blue) was added. Joint molecules were analyzed by electrophoresis in 1% agarose−TAE (40 mM Tris-acetate, pH 8.0, and 1 mM EDTA) gels and quantified using a Storm 840 phosphorimager (GE Healthcare), or joint molecules were passed twice through S-400 spin columns (GE Healthcare) equilibrated with 25 mM Tris-acetate, pH 7.5, at 23 °C and used as substrates in branch migration reactions.[50,51]

Branch Migration Assay. For RAD51-promoted reaction, RAD51 (1 μM) was incubated with **1** in the indicated concentrations in buffer containing 30 mM Tris-HCl, pH 7.5, 10 mM $MgCl_2$, 350 mM NaCl, 2 mM DTT, 2 mM ATP, 8 mM phosphocreatine, and 8 units/mL creatine phosphokinase for 30 min at 37 °C. Branch migration was initiated by addition of ^{32}P-labeled 3′-joint molecules (0.1 nM, molecules) that were produced by RAD51-promoted reaction (see above) and was carried out for 8 h. For RecA-promoted reaction, RecA (1 μM) was incubated with **1** in the indicated concentrations in buffer containing 25 mM Tris acetate, pH 7.5, 15 mM magnesium acetate, 2 mM DTT, 2 mM ATP, 10 mM phosphocreatine, and 10 units/mL creatine phosphokinase for 30 min at 37 °C. Branch migration was initiated by addition of ^{32}P-labeled 5′-joint molecules (0.1 nM, molecules) that were produced by RecA-promoted reaction (see above) and was carried out for 30 min. The DNA products were deproteinized and analyzed in 1.5% agarose−TAE gels and quantified using a Storm 840 phosphorimager (GE Healthcare).

D-Loop Assay. RAD51 (0.3 μM) was incubated with a 90-mer ^{32}P-labeled ssDNA (oligo 90) (0.9 μM, nt) in buffer containing 25 mM Tris-acetate (pH 7.5), 1 mM ATP, 1 mM $CaCl_2$, 100 μg mL^{-1} BSA, 1 mM DTT, and 20 mM KCl (added with the protein stock) for indicated periods at 37 °C. **1** (20 μM) was added to the mixture as indicated in Figure 2. D-Loop formation was initiated by addition of pUC19 supercoiled dsDNA (15 μM) and was carried out for 15 min. The DNA products were deproteinized by treatment with the stop mix (1% SDS and 880 μg mL^{-1} proteinase K) for 15 min at 37 °C. Samples were mixed with 0.1 vol of loading buffer (70% glycerol, 0.1% bromophenol blue) and analyzed by electrophoresis in 1% agarose−TAE (40 mM Tris-acetate, pH 8.0, and 1 mM EDTA) gels. Gels were quantified using a Storm 840 phosphorimager (GE Healthcare). The yield was expressed as a percentage of the total plasmid DNA.

DNA Binding Assay. RAD51 (1.0 μM) was incubated with **1** (25 μM) in buffer containing 25 mM Tris-acetate (pH 7.5), 2 mM ATP, 100 μg mL^{-1} bovine serum albumin (BSA), 1 mM dithiothreitol (DTT), and 2 mM $CaCl_2$ for 30 min at 37 °C.[21] Then a 90-mer ^{32}P-labeled ssDNA (oligo 90) (2.5 μM) and NaCl in indicated concentrations were added to the reaction mixture. After 10 min, 0.2 vol of 50% glycerol was added and the DNA products were analyzed by electrophoresis in 10% polyacrylamide gels (12 V/cm) in 0.5× TBE buffer (45 mM Tris borate, 0.25 mM EDTA, pH 8.3). Gels were dried on DE-81 paper and quantified using a Storm 840 phosphorimager (GE Healthcare).

dsDNA Coaggregation Assay. RAD51 protein (1 μM) was incubated with a 94-mer ssDNA (oligo 71) (3 μM, nt) in buffer containing 25 mM Tris-HCl, pH 7.5, 1 mM ATP, 100 μg/mL BSA, 1 mM DTT, 20 mM KCl (added with the protein stocks), and 2 mM $CaCl_2$ for 15 min at 37 °C. Then **1** (20 μM) was added to the mixture followed by NaCl in indicated concentrations, and coaggregation was initiated immediately by addition of ^{32}P-labeled linear pUC19 dsDNA (linearized by BamHI) (25 μM, nt). After a 10-min incubation at 37 °C, aliquots (10 μL) were withdrawn from the reaction mixture and coaggregates were collected by centrifugation in 0.5 mL Eppendorf tubes at 15000*g* for 5 min at 21 °C. Coaggregates were quantified using an LS 6500 liquid scintillation counter (Beckman). Residual retention of the radioactive DNA on the tube walls, ∼2−3% of total radioactivity, was subtracted.

ATPase Assay. RAD51 (1 μM) was incubated with **1** in indicated concentrations in buffer containing 25 mM Tris-acetate (pH 7.5), 1 mM DTT, 100 μg mL^{-1} BSA, 2 mM Mg acetate, 0.1 mM ATP, and 10 μCi [γ-^{32}P]ATP (6000 Ci $mmol^{-1}$) for 30 min at 37 °C. Then a 90-mer ssDNA (oligo 90) (3 μM, nt) was added to the reaction mixture. After 1.5 h the reactions were terminated by adding EDTA (100 mM) and the samples were analyzed by thin layer chromatography on polyethyleneimine cellulose strips (PEI-TLC) in 1 M formic acid/0.5 M LiCl. The inorganic [^{32}P]phosphate (P_i) released from [γ-^{32}P]ATP was quantified using a Storm 840 phosphorimager (GE Healthcare).

Measurement of 1 Binding to RAD51 by SPR. Experiments were performed using the ProteOn XPR36 SPR array system with ProteOn Manager software, version 3.0 (Bio-Rad), as described in Supporting Information.

RAD51 Foci Formation. The 2×10^5 log phase HEK-GFP cells were seeded in 3.5 cm tissue culture plates on glass coverslips pretreated with 0.01% poly-L-lysine (Sigma) and grown overnight. Then cells were incubated with **1** (50 μM) or without **1** for 2 h at 37 °C. Then cells were exposed to 0.5 Gy IR using a Primus linear accelerator (Siemens) at 6 mV, 3 Gy/min followed by a 2 h incubation at 37 °C. Cells were washed with phosphate-buffered saline (PBS) (8.1 mM Na_2HPO_4, 1.47 mM KH_2PO_4, 138 mM NaCl, and 2.7 mM KCl, pH 7.4), extracted with PBS containing 0.2% Triton X-100 and 1 mM phenylmethanesulfonyl fluoride (PMSF) for 5 min at 4 °C, and fixed with PBS supplemented with 3.0% formaldehyde and 2.0% sucrose for 10 min. Cells were permeabilized with PBS containing 0.5% Triton X-100 for 5 min and blocked with PBS containing 3% BSA and 0.05% Tween 20 for 30 min at 23 °C. Cells were treated with the polyclonal rabbit RAD51 antibodies (1:500 dilution) (a gift from Dr. Golub, Yale University) in PBS containing 3% BSA and 0.05% Triton X-100 overnight at 4 °C and then with Alexa Fluor 488 donkey antirabbit IgG (H + L) antibodies (1:1000 dilution) (Invitrogen) for 1 h at 23 °C followed by a 5 min staining with 500 ng/mL 4′,6-diamidino-2-phenylindole (DAPI) in PBS containing 0.05% Tween 20. Samples were washed in PBS containing 0.05% Tween 20, mounted in VectaShield (Vector Laboratories), and sealed with nail polish. The fluorescence images were obtained using an Olympus IX70 inverted microscope and iVision-Mac software (BioVision).

DR-GFP Assay. HEK-GFP cells were grown until the log phase (∼70% of confluence), harvested, and seeded in six-well plates (TPP) (precoated with 0.1% w/v poly- L-lysine) at a density of 4.5×10^5 cells/well; after 24 h **1** or **2** in indicated concentrations were added followed by a 1 h incubation at 37 °C. Then cells were transfected with pCBASce plasmid DNA encoding I-SceI endonuclease[29] using GenDrill (BamaGen BioScience). After 2 days of incubation, cells were analyzed by FACS using a Guava EasyCyte Plus system (Millipore).

Clonogenic Survival Assay. To measure the effect of **1** and DNA-damaging agents on cells the clonogenic survival assay was used.[52] MEF samples were seeded on 10 cm tissue culture dishes at densities of 2000 −10000 cells/dish and incubated overnight. When siRNA was used, HEK cells 24 h after siRNA transfection were seeded at densities of 2000−4000 cell/dish. Then **1** (5 μM), **3** (0.01 μM), or both reagents were added to cells for 1 h. Then MMC, cisplatin, or MMS was added to cells in indicated concentrations followed by 1 h of incubation for MEF or 2 h (unless indicated otherwise) for HEK cells. Cells were washed three times with PBS buffer and incubated in either DMEM+ or DMEM+ containing **1** (5 μM), **3** (0.01 μM), or both chemicals for 7−10 days or for an indicated period. Cells were fixed and stained using staining solution (0.05% crystal violet, 50% methanol in PBS). Colonies were counted using an AlphaImager 3400 with AlphaEaseFC, version 4.0, software (Alpha Innotech). The

percent of surviving cells was determined as described.[53] Untreated cells were used as a control; their survival was expressed as 100%.

■ ASSOCIATED CONTENT

Supporting Information

Supplementary methods, figures, and tables. This material is available free of charge via the Internet at http://pubs.acs.org.

■ AUTHOR INFORMATION

Corresponding Author

*Phone: 215-762-7195. Fax: 215-762-4452, E-mail: amazin@drexelmed.edu.

Notes

The authors declare no competing financial interest.

■ ACKNOWLEDGMENTS

We thank J. Clifford for pCBASce, pMX-GFP plasmid DNA, and HEK-GFP cells; A. Astrinidis for *Tp53*$^{-/-}$ MEF; E. Golub for RAD51 antibodies; and K. Beishline and D. Keene for help with RAD51 foci visualization. This work was supported by NIH Grants CA100839 and MH084119 (to A.V.M.) and 1R21AI087388 (to S.C.) and by the Leukemia and Lymphoma Society Scholar Award 1054-09 (to A.V.M.).

■ ABBREVIATIONS USED

HR, homologous recombination; DSB, DNA double-strand break; ICL, interstrand cross-link; dsDNA, double-strand DNA; ssDNA, single-strand DNA; MMC, mitomycin C; IR, ionizing radiation; HEK, human embryonic kidney (cell line 293); MEF, mouse embryonic fibroblast; PARP1, poly(ADP-ribose) polymerase 1; MMS, methyl methanesulfonate; GFP, green fluorescent protein; BER, base excision repair

■ REFERENCES

(1) Krogh, B. O.; Symington, L. S. Recombination proteins in yeast. *Annu. Rev. Genet.* **2004**, *38*, 233−271.
(2) Moynahan, M. E.; Jasin, M. Mitotic homologous recombination maintains genomic stability and suppresses tumorigenesis. *Nat. Rev. Mol. Cell Biol.* **2010**, *11*, 196−207.
(3) San Filippo, J.; Sung, P.; Klein, H. Mechanism of eukaryotic homologous recombination. *Annu. Rev. Biochem.* **2008**, *77*, 229−257.
(4) Agarwal, S.; Tafel, A. A.; Kanaar, R. DNA double-strand break repair and chromosome translocations. *DNA Repair* **2006**, *5*, 1075−1081.
(5) Mimitou, E. P.; Symington, L. S. DNA end resection: many nucleases make light work. *DNA Repair (Amst)* **2009**, *8*, 983−995.
(6) Kowalczykowski, S. C. Structural biology: snapshots of DNA repair. *Nature* **2008**, *453*, 463−466.
(7) Rossi, M. J.; Mazina, O. M.; Bugreev, D. V.; Mazin, A. V. The RecA/RAD51 protein drives migration of Holliday junctions via polymerization on DNA. *Proc. Natl. Acad. Sci. U.S.A.* **2011**, *108*, 6432−6437.
(8) Pâques, F.; Haber, J. E. Multiple pathways of recombination induced by double-strand breaks in *Saccharomyces cerevisiae*. *Microbiol. Mol. Biol. Rev.* **1999**, *63*, 349−404.
(9) West, S. C. The search for a human Holliday junction resolvase. *Biochem. Soc. Trans.* **2009**, *37*, 519−526.
(10) Symington, L. S.; Holloman, W. K. Resolving resolvases: the final act? *Mol. Cell* **2008**, *32*, 603−604.
(11) Tsuzuki, T.; Fujii, Y.; Sakumi, K.; Tominaga, Y.; Nakao, K.; Sekiguchi, M.; Matsushiro, A.; Yoshimura, Y.; Morita, T. Targeted disruption of the Rad51 gene leads to lethality in embryonic mice. *Proc. Natl. Acad. Sci. U.S.A.* **1996**, *93*, 6236−6240.
(12) Lim, D. S.; Hasty, P. A mutation in mouse rad51 results in an early embryonic lethal that is suppressed by a mutation in p53. *Mol. Cell. Biol.* **1996**, *16*, 7133−7143.
(13) Morrison, C.; Shinohara, A.; Sonoda, E.; Yamaguchi-Iwai, Y.; Takata, M.; Weichselbaum, R. R.; Takeda, S. The essential functions of human Rad51 are independent of ATP hydrolysis. *Mol. Cell. Biol.* **1999**, *19*, 6891−6897.
(14) Stark, J. M.; Hu, P.; Pierce, A. J.; Moynahan, M. E.; Ellis, N.; Jasin, M. ATP hydrolysis by mammalian RAD51 has a key role during homology-directed DNA repair. *J. Biol. Chem.* **2002**, *277*, 20185−20194.
(15) Forget, A. L.; Loftus, M. S.; McGrew, D. A.; Bennett, B. T.; Knight, K. L. The human Rad51 K133A mutant is functional for DNA double-strand break repair in human cells. *Biochemistry* **2007**, *46*, 3566−3575.
(16) Helleday, T.; Lo, J.; van Gent, D. C.; Engelward, B. P. DNA double-strand break repair: From mechanistic understanding to cancer treatment. *DNA Repair* **2007**, *6*, 923−935.
(17) Kawasumi, M.; Nghiem, P. Chemical genetics: elucidating biological systems with small-molecule compounds. *J. Invest. Dermatol.* **2007**, *127*, 1577−1584.
(18) Li, Y.; He, Y.; Luo, Y. Crystal structure of an archaeal Rad51 homologue in complex with a metatungstate inhibitor. *Biochemistry* **2009**, *48*, 6805−6810.
(19) Ishida, T.; Takizawa, Y.; Kainuma, T.; Inoue, J.; Mikawa, T.; Shibata, T.; Suzuki, H.; Tashiro, S.; Kurumizaka, H. DIDS, a chemical compound that inhibits RAD51-mediated homologous pairing and strand exchange. *Nucleic Acids Res.* **2009**, *37*, 3367−3376.
(20) Huang, F.; Motlekar, N. A.; Burgwin, C. M.; Napper, A. D.; Diamond, S. L.; Mazin, A. V. Identification of Specific Inhibitors of Human RAD51 Recombinase Using High-Throughput Screening. *ACS Chem. Biol.* **2011**, *6*, 628−635.
(21) Bugreev, D. V.; Golub, E. I.; Stasiak, A. Z.; Stasiak, A.; Mazin, A. V. Activation of human meiosis-specific recombinase Dmc1 by Ca^{2+}. *J. Biol. Chem.* **2005**, *280*, 26886−26895.
(22) Mazin, A. V.; Kowalczykowski, S. C. The function of the secondary DNA-binding site of RecA protein during DNA strand exchange. *EMBO J.* **1998**, *17*, 1161−1168.
(23) Howard-Flanders, P.; West, S. C.; Rusche, J. R.; Egelman, E. H. Molecular mechanisms of general genetic recombination: the DNA-binding sites of RecA protein. *Cold Spring Harbor Symp. Quant. Biol.* **1984**, *49*, 571−580.
(24) Tsang, S. S.; Chow, S. A.; Radding, C. M. Networks of DNA and RecA protein are intermediates in homologous pairing. *Biochemistry* **1985**, *24*, 3226−3232.
(25) Mazina, O. M.; Mazin, A. V. Human Rad54 protein stimulates DNA strand exchange activity of hRad51 protein in the presence of Ca^{2+}. *J. Biol. Chem.* **2004**, *279*, 52042−52051.
(26) Bugreev, D. V.; Mazina, O. M.; Mazin, A. V. Bloom syndrome helicase stimulates RAD51 DNA strand exchange activity through a novel mechanism. *J. Biol. Chem.* **2009**, *284*, 26349−26359.
(27) Haaf, T.; Golub, E. I.; Reddy, G.; Radding, C. M.; Ward, D. C. Nuclear foci of mammalian Rad51 recombination protein in somatic cells after DNA damage and its localization in synaptonemal complexes. *Proc. Natl. Acad. Sci. U.S.A.* **1995**, *92*, 2298−2302.
(28) Raderschall, E.; Golub, E. I.; Haaf, T. Nuclear foci of mammalian recombination proteins are located at single-stranded DNA regions formed after DNA damage. *Proc. Natl. Acad. Sci. U.S.A.* **1999**, *96*, 1921−1926.
(29) Pierce, A. J.; Johnson, R. D.; Thompson, L. H.; Jasin, M. XRCC3 promotes homology-directed repair of DNA damage in mammalian cells. *Genes Dev.* **1999**, *13*, 2633−2638.
(30) Menear, K. A.; Adcock, C.; Boulter, R.; Cockcroft, X. L.; Copsey, L.; Cranston, A.; Dillon, K. J.; Drzewiecki, J.; Garman, S.; Gomez, S.; Javaid, H.; Kerrigan, F.; Knights, C.; Lau, A.; Loh, V. M. Jr.; Matthews, I. T.; Moore, S.; O'Connor, M. J.; Smith, G. C.; Martin, N. M. 4-[3-(4-Cyclopropanecarbonylpiperazine-1-carbonyl)-4-fluorobenzyl]-2*H*-phthalazin-1-one: a novel bioavailable inhibitor of poly(ADP-ribose) polymerase-1. *J. Med. Chem.* **2008**, *51*, 6581−6591.

(31) Ito, M.; Yamamoto, S.; Nimura, K.; Hiraoka, K.; Tamai, K.; Kaneda, Y. Rad51 siRNA delivered by HVJ envelope vector enhances the anti-cancer effect of cisplatin. *J. Gene Med.* **2005**, *7*, 1044−1052.
(32) Ohnishi, T.; Taki, T.; Hiraga, S.; Arita, N.; Morita, T. In vitro and in vivo potentiation of radiosensitivity of malignant gliomas by antisense inhibition of the RAD51 gene. *Biochem. Biophys. Res. Commun.* **1998**, *245*, 319−324.
(33) Ko, J. C.; Hong, J. H.; Wang, L. H.; Cheng, C. M.; Ciou, S. C.; Lin, S. T.; Jheng, M. Y.; Lin, Y. W. Role of repair protein Rad51 in regulating the response to gefitinib in human non-small cell lung cancer cells. *Mol. Cancer Ther.* **2008**, *7*, 3632−3641.
(34) Sung, P.; Krejci, L.; Van Komen, S.; Sehorn, M. G. Rad51 recombinase and recombination mediators. *J. Biol. Chem.* **2003**, *278*, 42729−42732.
(35) Hu, Y.; Raynard, S.; Sehorn, M. G.; Lu, X.; Bussen, W.; Zheng, L.; Stark, J. M.; Barnes, E. L.; Chi, P.; Janscak, P.; Jasin, M.; Vogel, H.; Sung, P.; Luo, G. RECQL5/Recql5 helicase regulates homologous recombination and suppresses tumor formation via disruption of Rad51 presynaptic filaments. *Genes Dev.* **2007**, *21*, 3073−3084.
(36) Bugreev, D. V.; Yu, X.; Egelman, E. H.; Mazin, A. V. Novel pro- and anti-recombination activities of the Bloom's syndrome helicase. *Genes Dev.* **2007**, *21*, 3085−3094.
(37) Conway, A. B.; Lynch, T. W.; Zhang, Y.; Fortin, G. S.; Fung, C. W.; Symington, L. S.; Rice, P. A. Crystal structure of a Rad51 filament. *Nat. Struct. Mol. Biol.* **2004**, *11*, 791−796.
(38) Matsuo, Y.; Sakane, I.; Takizawa, Y.; Takahashi, M.; Kurumizaka, H. Roles of the human Rad51 L1 and L2 loops in DNA binding. *FEBS J.* **2006**, *273*, 3148−3159.
(39) Miyazaki, T.; Bressan, D. A.; Shinohara, M.; Haber, J. E.; Shinohara, A. In vivo assembly and disassembly of Rad51 and Rad52 complexes during double-strand break repair. *EMBO J.* **2004**, *23*, 939−949.
(40) Cer, R. Z.; Mudunuri, U.; Stephens, R.; Lebeda, F. J. IC50-to-Ki: a Web-based tool for converting IC50 to Ki values for inhibitors of enzyme activity and ligand binding. *Nucleic Acids Res.* **2009**, *37*, W441−W445.
(41) Sonoda, E.; Sasaki, M. S.; Buerstedde, J. M.; Bezzubova, O.; Shinohara, A.; Ogawa, H.; Takata, M.; Yamaguchi-Iwai, Y.; Takeda, S. Rad51-deficient vertebrate cells accumulate chromosomal breaks prior to cell death. *EMBO J.* **1998**, *17*, 598−608.
(42) Begg, A. C.; Stewart, F. A.; Vens, C. Strategies to improve radiotherapy with targeted drugs. *Nat. Rev. Cancer* **2011**, *11*, 239−253.
(43) Starcevic, D.; Dalal, S.; Sweasy, J. B. Is there a link between DNA polymerase beta and cancer? *Cell Cycle* **2004**, *3*, 998−1001.
(44) Neijenhuis, S.; Verwijs-Janssen, M.; van den Broek, L. J.; Begg, A. C.; Vens, C. Targeted radiosensitization of cells expressing truncated DNA polymerase {beta}. *Cancer Res.* **2010**, *70*, 8706−8714.
(45) Raderschall, E.; Stout, K.; Freier, S.; Suckow, V.; Schweiger, S.; Haaf, T. Elevated levels of Rad51 recombination protein in tumor cells. *Cancer Res.* **2002**, *62*, 219−225.
(46) Xia, S. J.; Shammas, M. A.; Shmookler Reis, R. J. Elevated recombination in immortal human cells is mediated by HsRAD51 recombinase. *Mol. Cell. Biol.* **1997**, *17*, 7151−7158.
(47) Maacke, H.; Opitz, S.; Jost, K.; Hamdorf, W.; Henning, W.; Kruger, S.; Feller, A. C.; Lopens, A.; Diedrich, K.; Schwinger, E.; Sturzbecher, H. W. Over-expression of wild-type Rad51 correlates with histological grading of invasive ductal breast cancer. *Int. J. Cancer* **2000**, *88*, 907−913.
(48) Henricksen, L. A.; Umbricht, C. B.; Wold, M. S. Recombinant replication protein A: expression, complex formation, and functional characterization. *J. Biol. Chem.* **1994**, *269*, 11121−11132. Published erratum: *J. Biol. Chem.* **1994**, *269*, 16519.
(49) Bugreev, D. V.; Mazina, O. M.; Mazin, A. V. Analysis of branch migration activities of proteins using synthetic DNA substrates. *Nat. Protoc.* DOI: 2010.1038/nprot.2006.2217. Published Online: September 1, **2006**.
(50) Rossi, M. J.; Mazina, O. M.; Bugreev, D. V.; Mazin, A. V. Analyzing the branch migration activities of eukaryotic proteins. *Methods* **2010**, *51*, 336−346.
(51) Bugreev, D. V.; Mazina, O. M.; Mazin, A. V. Rad54 protein promotes branch migration of Holliday junctions. *Nature* **2006**, *442*, 590−593.
(52) Essers, J.; Hendriks, R. W.; Swagemakers, S. M.; Troelstra, C.; de Wit, J.; Bootsma, D.; Hoeijmakers, J. H.; Kanaar, R. Disruption of mouse RAD54 reduces ionizing radiation resistance and homologous recombination. *Cell* **1997**, *89*, 195−204.
(53) Hall, E. J.; Giaccia, A. J. *Radiobiology for the Radiologist*, 6th ed.; Lipincott Williams & Wilkins: Philadelphia, PA, 2005.